Development of a light-responsive fluorinated poly(arylene ether) copolymer containing azobenzene groups in the main polymer chain

Journal:	*Molecular Systems Design & Engineering*
Manuscript ID	ME-ART-09-2023-000150.R1
Article Type:	Paper
Date Submitted by the Author:	01-Nov-2023
Complete List of Authors:	Tkachenko, Ihor; National Academy of Sciences of Ukraine, Department of Chemistry of Oligomers and Netted Polymers Kurioz, Yuriy; Institute of Physics National Academy of Sciences of Ukraine Kravchuk, Ruslan; Institute of Physics National Academy of Sciences of Ukraine; Institute of Physical Chemistry PAS Tolstov, Olexandr; National Academy of Sciences of Ukraine Department of Chemistry Glushchenko, Anatoliy; University of Colorado, Department of Physics Nazarenko, Vassili; Institute of Physics National Academy of Sciences of Ukraine; Institute of Physical Chemistry PAS Shevchenko, Valery; National Academy of Sciences of Ukraine Department of Chemistry

Design, System, Application

A novel fluorinated aromatic polyether featuring azobenzene fragments in the backbone is developed. Our design approach bases on azobenzenes as versatile light sensitive units while harnessing the exceptional thermostability conferred by the fluorinated aromatic components. The combination of *meta*-isomeric units, flexible aromatic ether groups, and sites of contortion (non-coplanar units of octafluorobiphenylene) within macromolecular chains results in a polymer with exceptional solubility and film-forming capabilities, setting the stage for its versatile applications. In the obtained polymer the *trans-cis-trans* photoisomerization of azobenzene switches occurs both in the solution and in the solid state. As well, it also exhibits the remarkable ability of its azobenzene fragments to orient under light illumination (linearly polarized green light). Exploring this research vividly highlights the potential of the developed fluorinated azo-polymer in advancing smart, light-driven materials, including reconfigurable photonic elements, optical switching, signal processing, laser technology, and actuation.

Molecular Systems Design & Engineering

ARTICLE

Development of a light-responsive fluorinated poly(arylene ether) copolymer containing azobenzene groups in the main polymer chain

Received 00th January 20xx,
Accepted 00th January 20xx

DOI: 10.1039/x0xx00000x

Ihor M. Tkachenko,*[a] Yuriy I. Kurioz, [b] Ruslan M. Kravchuk, [b,c] Olexandr L. Tolstov, [a] Anatoliy V. Glushchenko, [d] Vassili G. Nazarenko [b,c] and Valery V. Shevchenko [a]

A novel light-responsive poly(arylene ether) copolymer with both azobenzene and perfluorinated biphenylene units as well as meta-linked fragments in the main polymer chain is synthesized. The copolymer is synthesized using aromatic nucleophilic substitution reaction from decafluorobiphenyl and two dihydroxyl-substituted monomers, fluorinated bis-azobenzene-based phenol derivative, and resorcinol. The chemical structure of the copolymer is characterized using ^{1}H, ^{19}F NMR, FTIR, Raman and UV/vis spectroscopy techniques. The polymer shows remarkable solubility in organic solvents resulting in the formation of robust, self-supporting films. It displays impressive mechanical characteristics as well as remarkable resistance to thermo-oxidative degradation. Under UV light irradiation, photoisomerization occurs both in solution and in the solid copolymer film. The solid polymer films exhibit intense and stable birefringence changes upon the irradiation, enabling the fabrication of diffraction gratings. The study indicates that this synthetic approach is a simple and effective method for designing light-responsive materials.

Introduction

Considerable effort has been made to design, synthesize, and functionalize poly(arylene ether)s (PAEs) with different chemical compositions and applications in various areas.[1-5] Among the functional PAEs, azobenzene-based polyethers provide a versatile platform for developing thermo- and mechanically-stable materials with macroscopic properties that can be manipulated by light, making them highly functional.[6,7] These light-powered functional polymeric systems, capable of undergoing efficient and reversible photochemical reactions of azo groups to switch between trans (or E)- and cis (or Z)-isomers with markedly different properties, continue to impact the materials world.[8-11] Several studies have focused on the design of azobenzene-containing PAEs, including poly(arylene ether sulfone)s and poly(arylene ether ketone)s. As a result, a series of azobenzene-containing side-chain PAEs with reversible photoinduced birefringence and quick photoinduced surface-relief-grating formation ability are successfully synthesized.[12-15] Additionally, a new family of nonlinear optical (NLO) active PAEs bearing azo-chromophore derivatives as side chains are fabricated.[7,16] Main chain type azo-based PAEs are also used to form clear and stable surface relief gratings[17] and for fabricating fluorescent micropatterns.[18] Moreover, recent studies show that poly(arylene ether)s containing azobenzene groups in the main chain can undergo self-recoverable photoinduced deformation behavior.[6,19,20] Interestingly, Song and co-workers demonstrated that designing PAEs with rigid and contorted molecular structures (referred to as the "PIMs concept") is a helpful strategy to increase the polymer's free volume, thereby increasing the photoinduced deformation rates of the polymers. Finally, crosslinked materials based on azobenzene-containing PAEs with stable photoinduced optical anisotropy are developed.[21]

Despite significant advances in the chemistry of azo-based PAEs, the importance of azo-containing PAEs with perfluorinated aromatic fragments (FPAEs) is somewhat neglected in the literature. However, azo-free FPAEs themselves possess unique properties that are essential for effective functioning in modern high-tech applications, particularly in microelectronics,[22-24] optical telecommunications,[25-27] and fuel cell membrane technology.[28-30] In addition to the expected improvement in chemical and thermal stability, the introduction of perfluorinated aromatic units into the polymer structure allows for upgrading their optical and electro-optical properties, particularly to reduce refractive index and optical losses and to increase hyperpolarization. To enhance NLO efficiency and thermal stability, Delair et al. describe the synthesis and characterization of FPAEs (with perfluorinated aromatic units) functionalized with different NLO azo-chromophores as pendant groups.[7] Moreover, azo-based aromatic polymers with perfluorinated aromatic units and aromatic ether bonds are known, but their synthesis proceeds through the formation of urethane, imine, and other chemical bonds rather than ether linkages.[31-33]

The current study introduces a novel approach to designing an azo-containing copolymer with azobenzene and octafluorobiphenylene fragments in the main chain, Azo-coFPAE. The synthesis of Azo-coFPAE is straightforward, resulting in a polymer with good solubility, excellent mechanical properties,

[a] Institute of Macromolecular Chemistry, National Academy of Sciences of Ukraine, Kharkivske Shosse 48, Kyiv 02160, Ukraine. E-mail: ttkachenkoim@gmail.com
[b] Institute of Physics, National Academy of Sciences of Ukraine, Prospect Nauky 46, Kyiv, 03028, Ukraine.
[c] Institute of Physical Chemistry, PAS, Kasprzaka 44/52, 01-224 Warsaw, Poland.
[d] Department of Physics, University of Colorado at Colorado Springs, 1420 Austin Bluffs Parkway, Colorado Springs, CO 80918, USA.

profound thermal stability, and a high optical response. A systematic set of investigations is conducted on the chemical structure, mechanical and thermal properties, photoinduced birefringence, and photoisomerization behaviors (in both solution and film) of the synthesized Azo-coFPAE.

Experimental

Materials

Decafluorobiphenyl (3) (99%), 3-aminophenol (98%) and resorcinol (4) (99%) are purchased from Aldrich Chemical Co. and used as received. Anhydrous potassium carbonate (K_2CO_3, 99%) is purchased from Acros Organic Inc and dried at 120 °C for 24 hours before it is used. All the organic solvents are obtained from commercial sources and purified by conventional methods.

Synthesis of 3,3'-[(2,2',3,3',5,5',6,6'-octafluorobiphenyl-4,4'-diyl)bis(oxy)]dianiline (1). The target monomer **1** is synthesized according to the modified literature method.[34] The modified general procedure is followed: decafluorobiphenyl (5.00 g, 14.965 mmol), 3-aminophenol (3.35 g, 30.678 mmol), K_2CO_3 (4.12 g, 29.930 mmol), and DMSO (30 ml) are mixed, and the solution is stirred at 120°C for 6 hours. The mixture is allowed to cool to room temperature and filtered. The filtrate is poured into water. The white solid is obtained by filtration (yield 90%). ^{1}H NMR (DMSO-d_6, δ, ppm): 5.49 (br.s, 4H, NH_2), 6.28 (d, 2H, *J* = 7.8 Hz, Ar), 6.32 (s, 2H, Ar), 6.37 (d, 2H, *J* = 7.8 Hz, Ar), 7.02 (t, 2H, *J* = 7.8 Hz, Ar). Melting point: 137–138°C, which is consistent with the literature data.[34]

Synthesis of 4,4'-{(2,2',3,3',5,5',6,6'-octafluorobiphenyl-4,4'-diyl)bis[oxy-3,1-phenylenediazene-2,1-diyl]}diphenol (2). Azo-containing dihydroxyl-substituted monomer 2 is produced using the same procedure as in our previous paper.[35] The diamine **1** (1.00 g, 1.952 mmol) is suspended in 2.39 g of 18% HCl. The obtained mixture is stirred and cooled up to -5 °C. Sodium nitrite solution in water (1.56 ml, 2.5 M) is added dropwise to the stirred solution. Then, the obtained corresponding diazonium salt is added to 0.37 g (3.904 mmol) of phenol in 3.9 ml 2N NaOH solution. After stirring for 2 hours, the reaction solution is acidified by aqueous hydrochloric acid. The formed precipitate is collected by filtration, washed with a large amount of water, dried, and purified by means of boiling in chloroform (yield 87%). ^{1}H NMR (DMSO-d_6, δ, ppm): 6.97 (d, 4H, *J* = 8,8 Hz, Ar), 7.42 (d, 2H, *J* = 7,8 Hz, Ar), 7.64 (m, 4H, Ar), 7.67 (d, 2H, *J* = 7.8 Hz, Ar), 7.82 (d, 4H, *J* = 8.8 Hz, Ar), 10.41 (s, 2H, OH). NMR spectral data is in accordance with literature values.

Synthesis of azo-containing FPAE copolymer (Azo-coFPAE). A dry, 25 mL three-necked flask equipped with an oil bath, a mechanical stirrer, a cold water condenser, an argon inlet/outlet, and a thermometer is charged with azo-based monomer **2** (0.264 g, 0.366 mmol), decafluorobiphenyl (0.250 g, 0.748 mmol), and 4.3 mL of N,N-dimethylacetamide (DMAc). After dissolving the monomers, anhydrous potassium carbonate (0.111 g, 0.804 mmol) is added to the flask. The solution is then heated to 90 °C and stirred vigorously at this temperature for 1 hour. A solution of resorcinol (0.040 g, 0.366 mmol) in DMAc (1 ml) is then added to the reaction mixture. The molar ratio of OH-based components to decafluorobiphenyl is 0.977:1 respectively. After an additional 2-hour reaction at 90°C, the reaction mixture is cooled to room temperature and poured into 30 mL of methanol containing a few drops of glacial acetic acid to precipitate the polymer. The precipitate is collected, dried, and dissolved in chloroform, filtered to remove any insoluble solid, and reprecipitated by adding the solution dropwise into methanol. The separated polymer is dried in vacuo at 60 °C overnight. Yield 88 %. ^{1}H NMR ($CDCl_3$, δ, ppm): 6.79 (d, 2H, *J*=7.8 Hz, Ar), 6.86 (s, 1H, Ar), 7.18 (m, 6H, Ar), 7.34 (br. s, 1H, Ar), 7.52-7.60 (m, 4H, Ar), 7.74 (d, 2H, *J*=6.8 Hz, Ar), 7.96 (d, 4H, *J*=7.3 Hz, Ar). ^{19}F NMR ($CDCl_3$, 376 MHz, δ, ppm): -153.03 (m, 12F, Ar-F), -137.98 (m, 12F, Ar-F). FTIR ν (cm^{-1}): 976, 1001 (C-F), 1229 (Ar-O-Ar), 1474 (C=C_{arom}), 1593 (Ar), 2800-3100 (CH).

Characterization

^{1}H and ^{19}F NMR spectra are recorded using a Bruker Avance instrument at room temperature in $CHCl_3$. Chemical shifts for ^{1}H NMR are given relative to chloroform (δ = 7.25 ppm). For ^{19}F NMR, chemical shifts are reported on a scale relative to $CFCl_3$. Fourier transform infrared (FTIR) spectra (4000–400 cm^{-1}) of the synthesized compounds are recorded on a TENSOR 37 spectrometer using KBr pellets. Raman measurements are performed using Renishaw RM series Raman systems equipped with a Leica DM LM optical microscope. The solid-state Renishaw Near-IR laser with line of λ_{ex} = 785.0 nm is used for excitation. The laser beam with 300 mW energy of excitation is focused by 50× objective on the sample surface in the line with size 4×18 μm. WiRE 2.0 software is used to get the micro-Raman spectra and to control all parameters of measurements. The accuracy of determination of the frequency of phonon bands is around 1.15 cm^{-1}. The spectra are recorded in region 1800 – 100 cm^{-1}. UV/vis spectra of the obtained compounds are recorded on a Shimadzu UV-2450 spectrophotometer. The intrinsic viscosity ([η]) of the polymer in DMAc at 25 °C is determined using an Ubbelohde viscometer. The molecular weight and polydispersity indices of the copolymer were determined by gel permeation chromatography (GPC) (Waters Breeze 1515 GPC system). Tetrahydrofuran was used as the eluent and polystyrene was used as a standard.

The polymer films are prepared for analysis by casting solutions (approximately 3-5% w/v) in DMAc or chloroform onto a glass petri dish (Ø = 6 cm). Tensile testing is conducted using an Instron 5543 universal tensile machine equipped with a 500 N load cell in accordance with ISO 527-A standards. The tests are carried out at a cross-head speed of 1 mm/min at room temperature. The polymer's structure in powder form is examined using wide-angle X-ray diffraction (WAXD) on a Proto instrument equipped with an X-ray tube containing a copper anode and nickel filter, operating at 30 kV and 20 mA. WAXD patterns are obtained over the 2θ range of 10° to 40°, corresponding to wave vector (q) values of 7.15 to 27.8 nm^{-1}.

Differential scanning calorimetry (DSC) analysis is performed using a TA Q200 instrument. The film sample is heated from 0 to 400 °C with a heating rate of 20 °C min^{-1} under an air atmosphere. The glass transition temperature of the sample is obtained from the second heating run as the midpoint of the heat capacity change. The thermo-oxidative destruction of the copolymer is studied using thermal gravimetric analysis (TGA) with a TA Instruments Q-50 apparatus (USA) in air. The heating rate of 20 °C/min within the temperature range from 25 to 700 °C is applied.

Photoisomerization experiments are conducted in solution and solid-state phases. In the solution phase, the sample is subjected to irradiation using a DeLux EBT-01 mercury lamp (26 W) emitting 365 nm UV light at a distance of 10 cm, followed by recording the resulting changes. Solid-state photoisomerization is performed on a polymer film by applying 365 nm UV light with a power density of 3-4 mW at a distance of 4 cm. Back-isomerization is induced by UV-visible light irradiation (250 to 700 nm) at a distance of 2.5 cm using a compact deuterium lamp with a power range of 8-12 mW.

To determine the photoinduced birefringence in the Azo-coFPAE film of thickness 18 µm, an experimental optical arrangement, as described in Ref.[31,36] is utilized. Specifically, the polymer film is subjected to irradiation with the polarized light of an Ar laser (λ = 532 nm, P_{max} = 50 mW) and is simultaneously positioned between the crossed polarizers of a He-Ne laser (λ = 628 nm, P_{max} = 5 mW) serving as a probe beam. The polarization direction of the irradiating light is set at 45° with respect to the orientation of the polarizer and analyzer. The variation in the sample's birefringence during irradiation, as a function of illumination time, is monitored. The diffraction gratings are formed using the experimental set-up described in Ref.[31,36]

Results and discussion

Synthesis and characterization of the main-chain Azo-coFPAE polymer

The required azo-containing hydroxyl-substituted monomer **2** with octafluorobiphenylene (OFB) central unit to the target azo-containing copolymeric FPAE (Azo-coFPAE) is prepared by simple diazotization reaction of aromatic *meta*-linked diamine **1** followed by azo coupling with phenol. The copolyether Azo-coFPAE is synthesized by the aromatic nucleophilic substitution reaction from DFB **3** and an equimolar amount of hydroxyl-substituted monomers **2** and **4** in DMAc in the presence of excess potassium carbonate as a base (**Fig. 1a**).

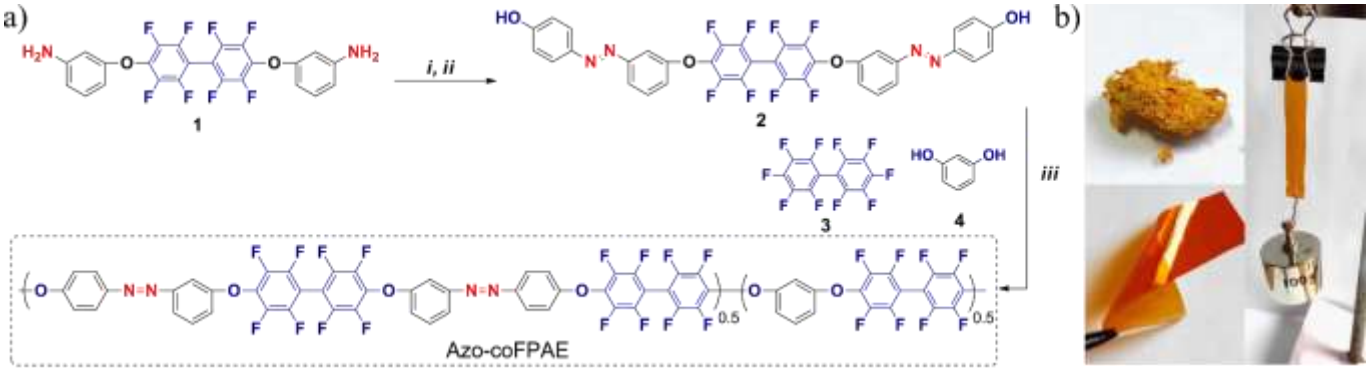

Fig. 1 (a) Synthetic route and chemical structures of the azo-based monomer (**2**) with an OFB central unit derived from diamine **1** and phenol, and corresponding *meta*-linked fluorinated copolymer Azo-coFPAE functionalized with photochromic azobenzene groups prepared via co-polycondensation of monomer **2** with DFB (**3**) and resorcinol (**4**). Reagents and conditions: (i) HCl, $NaNO_2$, -5 °C, 2 h; (ii) phenol, NaOH, 0-5 °C, 4 h, yield = 85%; (iii) DMAc, K_2CO_3, 90 °C, 3 h, yield =92 % after reprecipitation. (b) Azo-coFPAE fibers which are obtained by the precipitation of the reaction solution in cold methanol (top left panel), free-standing film of Azo-coFPAE, which is prepared by the solvent casting method using chloroform as the solvent (bottom left panel) and image of 70 mg Azo-coFPAE film with a load of 100 g weight (right panel): the load is fixed by a staple, thus the film is perforated.

The resulting Azo-coFPAE copolymer is isolated as an orange fibrous solid (**Fig. 1b**) that is found to be fully soluble in chloroform and DMAc but insoluble in alcohols. The intrinsic viscosity ([η]) of the polymer is measured to be 0.34 dL g^{-1}, in DMAc solutions containing at 25 °C. According to GPC results, the number-average molecular weight (M_n) and the polydispersity index (PDI) of the Azo-coFPAE were 17700 and 2.44, respectively (**Fig. S1**). The copolymer can be cast from the solution to form high-quality self-supporting films which are mechanically robust and can be easily handled (**Fig. 1b**). Note that DFB is the most used monomer in the synthesis of FPAEs. Eventually, OFB fragments are inserted into the structure of the polymer chains via both azo-based monomer **2** and DFB as a monomer. Importantly, OFB fragments have a significant impact on molecular packing and properties of the resulting polymers since the aromatic rings of OFB fragments are nonplanar and thus an OFB fragment provides a site of contortion due to the covalent bond (between perfluorinated phenylene fragments) about which there is restricted rotation.[37] We also include the isomeric *meta*-phenoxy units in the polymer chemical structure using resorcinol as a *meta*-linker and monomer **2** with azo groups in the *meta* position to the aromatic ether linkage. This choice is based on our previous results, which demonstrate that *meta*-connecting polymers possess enhanced solubility, thermostability and mechanical properties.[38]

The success of the synthesis of the Azo-coFPAE is confirmed with ^{1}H NMR, ^{19}F NMR, FTIR and Raman spectroscopy techniques. All peaks in the ^{1}H NMR spectrum of the representative copolyether Azo-coFPAE can be readily assigned to the protons in the corresponding repeat units (**Fig. S2a top**). ^{1}H NMR spectra of the synthesized polymers do not also show any signals corresponding to the terminal -OH groups of the initial monomers. With respect to ^{19}F NMR spectra, two peaks are detected in the spectrum of Azo-coFPAE corresponding to *ortho*- and *meta*-fluorine atoms of the perfluorinated biphenylene fragments (**Fig. S2a bottom**). The FTIR spectrum of copolymer shows peaks which correspond to C–F, -C-O-C-, -C=C_{arom}- and CH groups (**Fig. S2b**). Additionally, the FTIR spectrum of the obtained copolymer shows no sign of an intense broad band in the range of 3600–3100 cm^{-1} corresponding to OH groups and characteristic for the initial monomer (**Fig. S2b**). This indicates that these groups are consumed during the polycondensation reaction.

Vibration N=N bond stretching is not observed clearly by FTIR spectroscopy while in the Raman spectrum the corresponding band is more easily recognized by its high intensity.[39,40] **Fig. S2c** shows the Raman spectrum from 900 to 1750 cm^{-1} of the analyzed Azo-coFPAE. All Raman peaks below 900 cm^{-1} in the polymers are obscured by fluorescence.[40] In the Raman spectrum for Azo-coFPAE, the bands at 1435 and 1146 cm^{-1} are assigned as the N=N (v10) and C–N (v15) stretching vibrational modes of the azobenzene fragment, respectively.[41] The strong Raman band at 1001 cm^{-1} is mainly stemmed from the ring deformation mode of *meta*-linked aromatic rings.[42] The band at 1654 cm^{-1} may arise from C=C stretching of the OFB fragment since this band is also observable in the spectrum of DFB.[43] The band at 1595 cm^{-1} was assigned as C=C bond stretching mode of all the aromatic structures within the macromolecule. All the other modes are of mixed nature involving aromatic ring deformations (C=C, C=C(H) and C=C(F) modes), C–O, C–F, C–N and C–H stretching.

The wavelengths of absorption maximum (λ_{max}) in the UV/vis spectra of Azo-coFPAE both in chloroform and in more polar DMAc are around 336 nm, corresponding to the π-π* transition of the *trans*-azobenzene units (**Fig. 2a**). The absorption band at 444 nm, indicative of the n-π* electronic transition of azobenzenes, displays weaker intensity in the copolymer UV/vis spectrum in both solvents.

The slight broadening of the absorption band of Azo-coFPAE in chloroform relative to DMAc may suggest partial aggregation of the azobenzene chromophores. Unlike the copolymer, the monomer is not soluble in pure chloroform. Thus, a nonpolar chloroform is a poorer solvent compared to the polar DMAc for Azo-coFPAE, resulting in weaker solvation of the azobenzene chromophores.

While Azo-coFPAE shows the strong absorption band at around 336 nm, the azo-based monomer **2** of the phenolic type exhibits the band width maximum at 365 nm in DMAc (**Fig. 2b**). The observed bathochromic shift in the monomer's UV/vis spectrum, compared to the copolymer, can be attributed to the formation of hydrogen-bonded complexes between the OH groups of monomer **2** and DMAc (**Fig. S3a**). The formation of such complexes was studied in more detail in our work using the example of a fluorinated monomer with a similar structure to monomer **2**.[44] Additionally, comparing the FTIR spectra of monomer **2** in its solid state, pure DMAc, and the monomer **2**/DMAc mixture also reveals the formation of hydrogen-bonded complexes. The noticeable broadening of the 3700-3100 cm^{-1} band in the monomer **2**/DMAc spectrum, signifying OH group presence, and the shift of the characteristic C=O band of pure DMAc solvent (1647 cm^{-1}) to lower wavenumbers (1630 cm^{-1}) in the monomer **2**/DMAc mixture, support the formation of complexes between the OH group of monomer **2** and the C=O group of DMAc (**Fig. S3b**). These results are in agreement with the literature data.[44-47] Due to the formation of the monomer-solvent complex, the absorption band in the visible region (430-540 nm) is broad and intense, with a maximum at around 488 nm. This region also includes the n-π* transitions of azobenzene. When the solvent polarity is decreased by using a mixture of chloroform and DMAc, the monomer-solvent complex is partially disrupted. This results in a blue shift of the π-π* absorption to 354 nm, and a corresponding decrease in the intensity of the n-π* absorption (**Fig. 2b**).

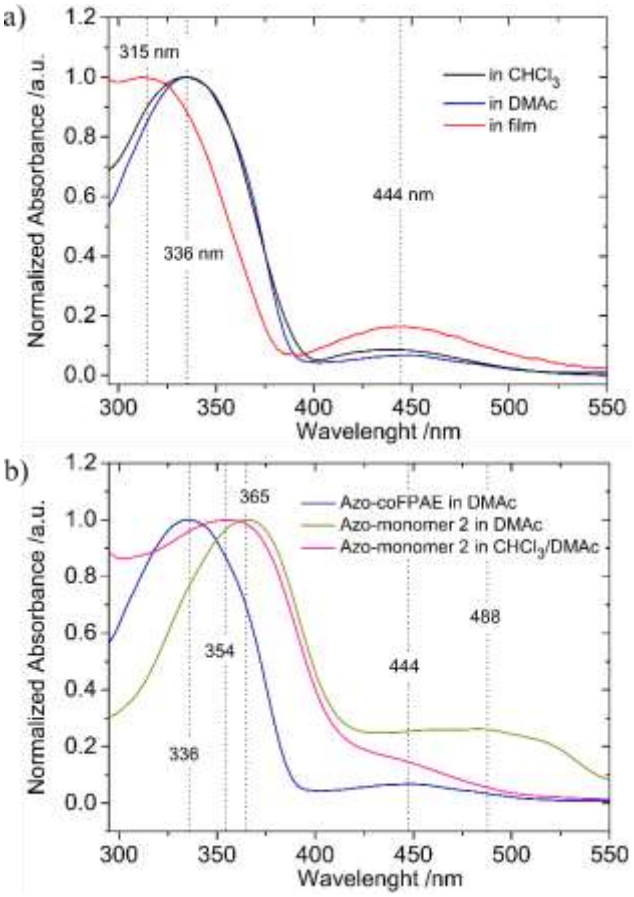

Fig. 2 (a) UV/vis absorbance spectra of Azo-coFPAE in $CHCl_3$, DMAc and solid film. (b) Comparison between the UV/vis absorbance spectra of azo-based monomer **2** (in DMAc and a mixture of $CHCl_3$ and DMAc (4/1, v/v)) and respective copolymer Azo-coFPAE in $CHCl_3$.

These results additionally suggest that the OH groups of the monomer **2** are fully involved in a polycondensation reaction.

Structure, thermal and mechanical properties

For polymer materials to be successfully applied in modern industry and technology, they must demonstrate excellent mechanical and thermal properties. Free-standing flexible and tough Azo-coFPAE film (**Fig. 1b**) is successfully prepared from chloroform for mechanical characterization. The tests reveal a tensile strength of about 62 MPa, Young's modulus of 1.45 GPa and elongation at break of 5 % of the Azo-coFPAE film.

Wide-angle X-ray diffraction (WAXD) measurements demonstrate that the Azo-coFPAE copolymer is amorphous. The WAXD pattern displays the single diffuse broad peak (an amorphous halo) centered around 2θ = 22.8° (**Fig. 3a**). According to Bragg's law, this peak corresponds to a *d*-spacing of 0.39 nm in the polymer sample. The measured value corresponds to the chain-to-chain distance between densely packed polymer chains within the material.

Thermal properties of the resulting Azo-coFPAE are investigated by DSC and TGA techniques. DSC measurements support the amorphous nature of the copolymer because no melting endotherm peak is found from the first and second heating DSC scans. The

polymer shows the glass transition temperature (T_g) at 149 °C (ΔC_p = 0.7015 J g^{-1} K^{-1}) within the glass transition region (ΔT_g) from 134 to 164 °C (**Fig. 3b**). Note, that the *cis*-rich azopolymers (after *trans* to *cis* switching) may have a significantly lower T_g value.[48-50]

Owing to the high content of fluorinated units, the copolymer has good thermal stability and exhibits a one-step pattern of decomposition. It demonstrates a temperature of 487°C at 5% weight loss ($T_{5\%}$), indicating its suitability for various applications (**Fig. 3c**).

The heat-resisting index (HRI) for Azo-coFPAE is calculated by the equation: $T_{HRI} = 0.49\times[T_{5\%}+0.6\times(T_{30\%} - T_{5\%})]$,[51] where $T_{30\%}$ is the decomposition temperature at 30% weight loss ($T_{30\%}$ = 561°C, see **Fig. 3c**). The corresponding T_{HRI} value of the Azo-coFPAE film is 260.4 °C. The findings indicate that the HRI value of the polymer remains consistently high, comparable to renowned heat-resistant polymers like polyimides,[51] as well as high-performance composites derived from polyarylene ether nitriles[52] or fluorinated phthalonitrile.[53]

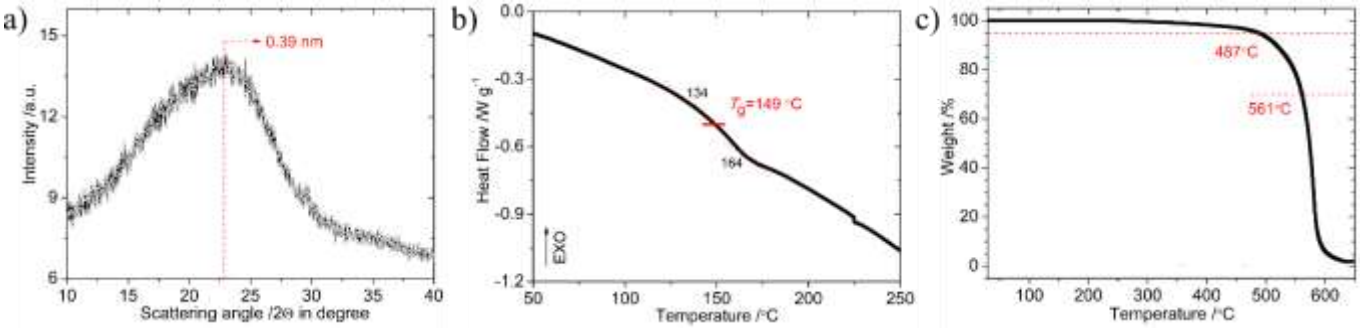

Fig. 3 (a) WAXD pattern, (b) DSC second heating cycle and (c) TGA curve of Azo-coFPAE copolymer.

Thus, the incorporation of rigid azobenzene units into the Azo-coFPAE polymer backbone leads to an approximate 20°C increase in the T_g value, but, as anticipated, it also results in a modest decrease in the $T_{5\%}$ value of about 50°C compared to FPAE based solely on DFB and resorcinol.[54]

Photoisomerization of Azo-coFPAE copolymer in solution and thin films

The photoisomerization capability of azobenzene-based compounds represents a highly versatile and dynamic approach for tailoring their properties to specific applications. We first investigate the photoswitching behavior of the synthesized Azo-coFPAE copolymer in a chloroform solution by monitoring the decay of the π-π* transition of *trans*-azobenzene at 336 nm (**Fig. 4a**).

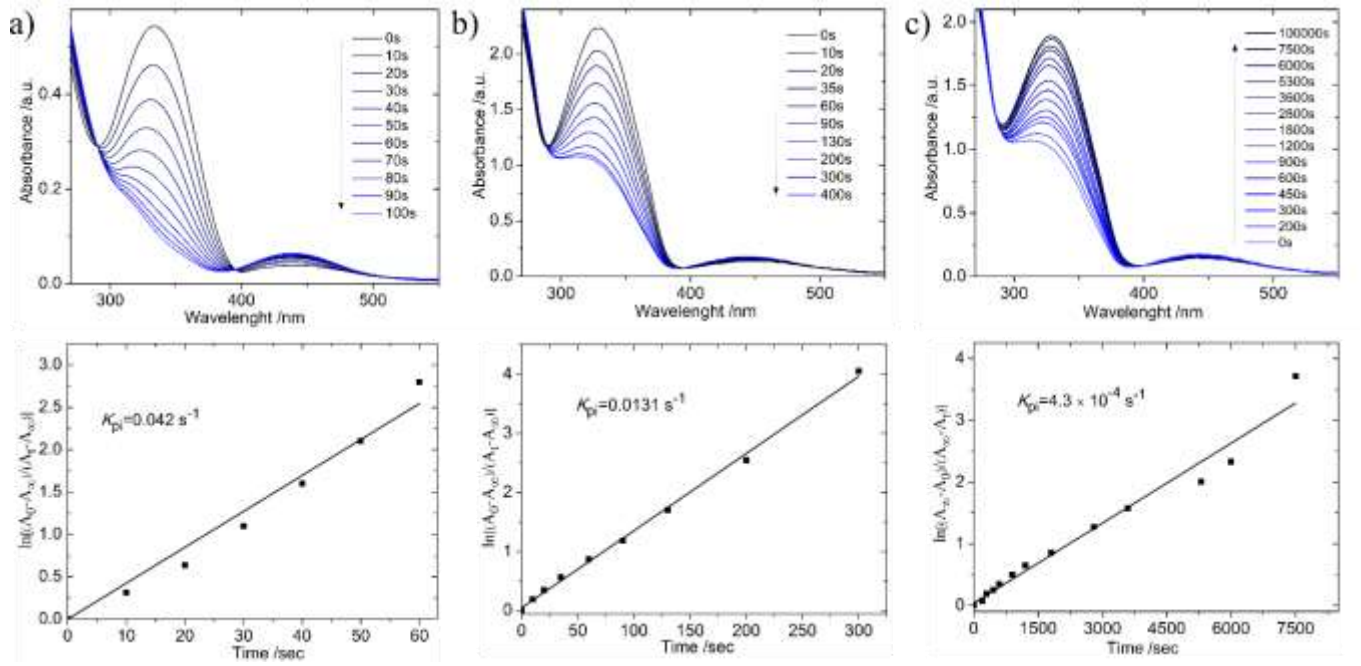

Fig. 4 (a) *Trans-cis* photoisomerization of Azo-coFPAE in $CHCl_3$ (top). Kinetic of the *trans-cis* photoisomerization of Azo-coFPAE in $CHCl_3$ (bottom). (b) *Trans-cis* photoisomerization of Azo-coFPAE in a thin film (λ = 365 nm, 3-4 mW) (top). Kinetic of the *trans-cis* photoisomerization of Azo-coFPAE in a thin film (bottom). (c) *Cis-trans* photoisomerization of Azo-coFPAE in a thin film (deuterium lamp, λ = 275±25 nm, 8-12 mW) (top). Kinetic of the *cis-trans* photoisomerization of Azo-coFPAE in a thin film (bottom).

The first-order rate constant of photoisomerization (K_{pi}) can be calculated from the slope of the plot of $\ln[(A_0 - A_\infty)/(A_t - A_\infty)]$ as a function of time.[6] In this equation A_0, A_∞, and A_t refer to the absorbances before irradiation, after reaching a photostationary state, and at a specific time during the process, respectively. We find that the value of constant K_{pi} for the Azo-coFPAE copolymer in chloroform solution reaches 0.0412 s^{-1}. As expected, the photoisomerization of Azo-coFPAE in a thin film is slower, with the observed rate constant K_{pi} of 0.0131 s^{-1} (**Fig. 4b**). The obtained K_{pi} values are comparable to the known rate constants for poly(arylene ether)s containing *bis*-azobenzene groups in the main chain.[6,20]

Upon comparing the extent of E-to-Z photoisomerization in solution and in the film, it is observed that a small portion of the azobenzene units remains in the *trans* form in the solid state when the photostationary state is achieved (about 400 s). In the solid state, cis isomers and the remaining trans isomers are stabilized, likely due to packing effects.[55,56] In a dilute chloroform solution, the majority of *trans* isomeric azobenzene fragments convert into *cis* isomers within just 70-80 s of irradiation (**Fig. 4a**).

Next, we study light-driven *cis-trans* isomerization by monitoring the recovery of *trans*-azobenzene unit's absorbance in an irradiated copolymer film sample. Photoinduced conversion between *trans* and *cis* configurations in copolymer proceeds almost completely in both directions. (**Fig. 4(b)** and **(c)**). The rate constant is obtained by plotting $\ln[(A_\infty - A_0)/(A_\infty - A_t)]$ versus time. The reconversion from the *cis*-form to the *trans*-form is achieved within several minutes by irradiating samples with white light. The rate constant of the reverse isomerization process is about 4.3×10^{-4} s^{-1}.

Birefringence measurements and diffraction grating writing

The photoinduced alignment of the azobenzene fragments perpendicular to the polarization direction of the incident light leads to the generation of birefringence in the polymer film upon illumination.[33,36] The optical response of the Azo-coFPAE film is investigated upon irradiation with polarized light (λ = 532 nm, P = (0.5 – 10) mW). The time-dependent photoinduced birefringence for copolymer, expressed in terms of transmission efficiency, is illustrated in **Fig. 5a**. The intensity of birefringence in the Azo-coFPAE film increases after the initiation of irradiation with polarized light, and at a certain point, it reaches a constant value (**Fig. 5a**). Following the termination of irradiating light, a relaxation process is observed. The residual birefringence ratio is calculated by dividing the residual birefringence by the maximum birefringence and is found to be 70% after approximately 300 seconds from the termination of excitation light, as depicted in **Fig. 5a**. The relatively fast birefringence relaxation is likely related to the flexible polyether backbone of the copolymer. Typically, the relaxation curve can be fitted with a bi-[57] or, more rarely, a tri-exponential function.[58,59]

The birefringence decay for Azo-coFPAE copolymer is well-fitted using three exponents (**Fig. 5a**, inset), indicating the presence of three distinct processes, two of which are fast (about 12.6 s for t_1 and t_2) and one that is slower (about 113.9 s for t_3). The "fast" decay can be attributed to the thermal *cis-trans* isomerization and dipole reorientation, while the "slow" process originates from the movement of the main chains.

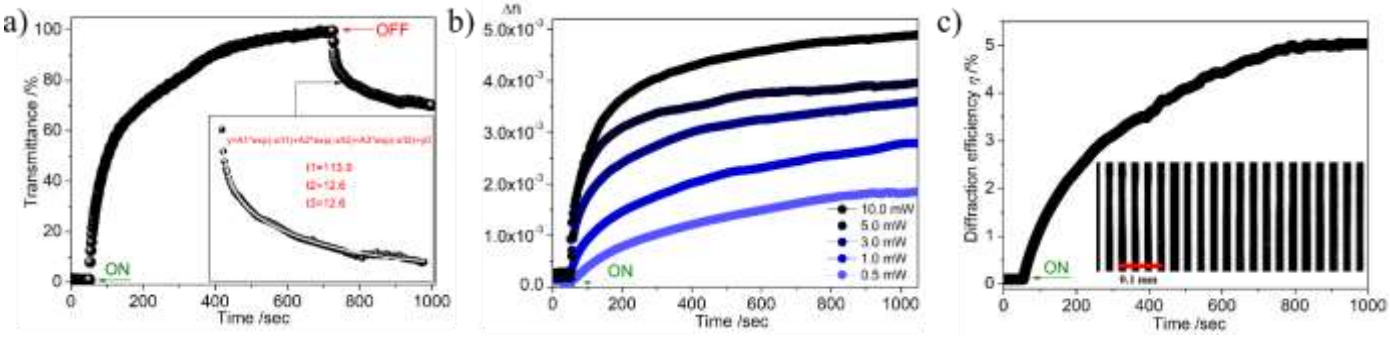

Fig. 5 (a) Kinetics curve for the buildup and relaxation of birefringence in Azo-coFPAE film (λ = 532 nm, P ~ 10 mW). Inset: the decay of birefringence after the writing laser is turned off, the relaxation is fitted by an exponential function, as shown by the white solid line. (b) Photoinduced birefringence curves for Azo-coFPAE film with a thickness of 18 μm as a function of the writing laser power (λ = 532 nm). (c) Dependency of diffraction efficiency for Azo-coFPAE film on irradiation time. Inset: photo of an Azo-coFPAE diffraction grating with a resolution of 30 lines per millimeter in a polarization microscope.

The level of birefringence in the Azo-coFPAE film is presented in **Fig. 5b**. The birefringence reaches values of approximately 5.0×10^{-3} for the following parameters of the experiment: λ = 532 nm, where laser power is 10 mW, film thickness is 18 μm. The measured value is close to the birefringence levels observed in analogous polymer systems with azobenzene groups in the backbone.[33] The polymer film derived from chloroform and the film obtained from DMAc demonstrate practically identical characteristics of light-induced birefringence.

The recording of a diffraction grating is also performed. In particular, the gratings are generated through the 2-beam irradiation of the films using a spatially modulated Ar laser (λ = 532 nm) with a power of 1.0 mW per beam.[31] A polarized microscope picture of the recorded diffraction grating on the Azo-coFPAE with a resolution of ~30 lines per millimeter is shown in **Fig. 5c** (inset). The value of diffraction efficiency, determined using the known formula, $\eta = (I_{+1}/I_0) \times 100\%$,[31] reaches a maximum value of approximately 5%, **Fig. 5c.** The recorded diffraction gratings are stable in time for several months.

Conclusions

This study explores a straightforward and effective synthetic method for preparing a novel copolyether, which contains azobenzene groups and perfluorinated biphenylene units in the main chains. The copolymer demonstrates exceptional solubility in highly polar solvents and even in chloroform, attributed to the presence of meta-linkages and non-coplanar fluorinated aromatic rings in the octafluorobiphenylene fragments. These structural features also contribute to the copolyether's excellent film-forming abilities and high thermo-oxidative stability. The study demonstrates that UV irradiation induces E-to-Z photoisomerization of the synthesized material in both chloroform solution and the solid state, while white light irradiation induces the reverse Z-to-E isomerization in the film, indicating a great potential for reversible photo-switching in this material. The photoorientation ability of azobenzene fragments in the copolymer film, when irradiated with a green laser, results in the acquisition of anisotropic properties by the film showcasing its potential for the fabrication of diffraction gratings.

Author contributions

Ihor M. Tkachenko: Investigation, Writing – original draft. Yuriy I. Kurioz: Investigation. Ruslan M. Kravchuk: Investigation. Olexandr L. Tolstov: Investigation. Anatoliy V. Glushchenko: Investigation, Writing – review & editing. Vassili G. Nazarenko: Writing – review & editing, Supervision, Resources, and Project administration. Valery V. Shevchenko: Conceptualization.

Conflicts of interest

There are no conflicts of interest to declare.

Acknowledgments

This work was supported by NASU project 0123U100832, NATO SPS project G6030 and by the Office of Naval Research Global Grant # N62909-23-1-2088. VN and RK thank the long-term program of support of the Ukrainian research teams at the PAS Polish Academy of Sciences carried out in collaboration with the U.S. National Academy of Sciences with the financial support of external partners via the agreement No. PAN.BFB.S.BWZ.356.022.2023. IT thanks the scholarship of the Verkhovna Rada of Ukraine for young scientists – doctors of science (No 0123U103605). YuK thanks the Johns Hopkins University - U4U Fellowship Program for support. We thank E. Zuyeva for graphical abstract design.

References

1. M.G. Dhara and S. Banerjee, *Progress in Polymer Science*, 2010, **35**, 1022-1077.
2. A. Hay, *Progress in Polymer Science*, 1999, **24**, 45-80.
3. K. Mazumder, H. Komber, E. Bittrich, B. Voit and S. Banerjee, *Macromolecules*, 2022, **55**, 1015-1029.
4. W. Huang, T. Ju, R. Li, Y. Duan, Y. Duan, J. Wei and L. Zhu, *Advanced Electronic Materials*, 2023, **9**, 2200414.
5. Y. Hu, B. Wang, X. Li, D. Chen and W. Zhang, *Journal of Power Sources*, 2018, **387**, 33-42.
6. Y. Zhang, J. Yuan, X. Zhao, L. Wu, Z. Liu and X.-M. Song, *Polymer Chemistry*, 2022, **13**, 569-576.
7. K. Aljoumaa, Y. Qi, J. Ding and J. A. Delaire, *Macromolecules*, 2009, **42**, 9275-9288.
8. M. Gao, D. Kwaria, Y. Norikane and Y. Yue, *Natural Sciences*, 2022, e220020.
9. M.M. Russew and S. Hecht, *Advanced Materials*, 2010, **22**, 3348-3360.
10. A.I. Bunea, D. Martella, S. Nocentini, C. Parmeggiani, R. Taboryski and D.S. Wiersma, *Advanced Intelligent Systems*, 2021, **3**, 2000256.
11. V.M. Ovdenko, D.O. Komarenko, S.O. Lisniak, A.V. Ronkovych, V.V. Multian and V.Y. Gayvoronsky, *Optical Materials*, 2023, **138**, 113735.
12. Y. Zhang, S. Pei, Y. Wang, Z. Cui, N. Li, Y. Zhu, H. Zhang and Z. Jiang, *Dyes and Pigments*, 2013, **99**, 1117-1123.
13. J. Zhang, H. Zhang, X. Chen, Y. Zhang, X. Li, Q. Chen and Z. Jiang, *Materials Letters*, 2010, **64**, 337-340.
14. J. Zhang, H. Zhang, X. Chen, J. Pang, Y. Zhang, Y. Wang, Q. Chen, S. Pei, W. Peng and Z. Jiang, *Reactive and Functional Polymers*, 2011, **71**, 553-560.
15. J. Zhang, H. Zhang, Q. Zhang, Z. Jiang, Q. Chen and Y. Zhang, *High Performance Polymers*, 2016, **28**, 518-524.
16. Y. Zhang, S. Gai, Z. Wang, S. Wang, A. Sui and X.-M. Song, *RSC Advances*, 2019, **9**, 9253-9259.
17. X. Jiang, X. Chen, X. Yue, J. Zhang, S. Guan, H. Zhang, W. Zhang and Q. Chen, *Reactive and Functional Polymers*, 2010, **70**, 616-621.
18. Y. Zhang, J. Zhang, Z. Cui, Q. Chen, H. Zhang and Z. Jiang, *Journal of Polymer Science Part A: Polymer Chemistry*, 2015, **53**, 936-943.
19. Y. Zhang, X. Zhao, J. Yuan, X. An, X. Sun, J. Yi and X.-M. Song, *Journal of Materials Chemistry C*, 2021, **9**, 14139-14145.
20. Y. Zhang, X. Sun, X. An, A. Sui, J. Yi and X.-M. Song, *Dyes and Pigments*, 2021, **186**, 109018.
21. Y. Zhang, S. Wang, Z. Wang, S. Gai and X.-M. Song, *Designed Monomers and Polymers*, 2017, **20**, 496-504.
22. C.-H. Chen, W.-F. Shiao, M. Ariraman, C.-H. Lin and T.-Y. Juang, *Polymer*, 2018, **151**, 307-315.
23. I. Tkachenko, Yu. Kononevich, Ya. Kobzar, O. Purikova, Yu. Yakovlev, I. Khalakhan, A. Muzafarov and V. Shevchenko, *Polymer*, 2018, **157**, 131-138.
24. L. Wang, M. Qu, Z. Wang, H. Wang, J. Zhao and G. Zhou, *Journal of Applied Polymer Science*, 2023, **140**, e53628.
25. K.-S. Lee, J.-P. Kim and J.-S. Lee, *Polymer*, 2010, **51**, 632-638.
26. Y. Wan, Y. Zhang, Z. Shi, W. Xu, X. Zhang, L. Zhao and Z. Cui, *Polymer*, 2012, **53**, 967-975.
27. J. Wang, G. Li, X. Jian and M. Zhao, *Polymer International*, 2012, **61**, 711-718.
28. O. Danyliv, C. Gueneau, C. Iojoiu, L. Cointeaux, A. Thiam, S. Lyonnard and J.-Y. Sanchez, *Electrochimica Acta*, 2016, **214**, 182-191.
29. X.Q. Wang, C.X. Lin, H.F. Liu, L. Li, Q. Yang, Q. Zhang, A. Zhu and Q.L. Liu, *Journal of Materials Chemistry A*, 2018.
30. K. Kallitsis, R. Nannou, A. Andreopoulou, M. Daletou, D. Papaioannou, S. Neophytides and J. Kallitsis, *Journal of Power Sources*, 2018, **379**, 144-154.
31. A.I. Kovalchuk, Ya.L. Kobzar, I.M. Tkachenko, Yu.I. Kurioz, O.G. Tereshchenko, O. V. Shekera, V.G. Nazarenko and V.V. Shevchenko, *Acs Applied Polymer Materials*, 2020, **2**, 455-463.

32. V. Shevchenko, A. Sidorenko, V. Bliznyuk, I. Tkachenko, O. Shekera, N. Smirnov, I. Maslyanitsyn, V. Shigorin, A. Yakimansky and V. Tsukruk, *Polymer*, 2013, **54**, 6516-6525.
33. I.M. Tkachenko, Yu.I. Kurioz, R.M. Kravchuk, O.V. Shekera, A.V. Glushchenko, V.G. Nazarenko and V.V. Shevchenko, *Polymer*, 2023, 125991.
34. A.E. Borodin and B.F. Malichenko, *Dopov Akad Nauk Ukr RSR Ser Geol Khim Biol*, 1978, 710-712.
35. V. Shevchenko, I. Tkachenko, A. Sidorenko and O. Shekera, *Dopov. Nac. Akad. Nauk Ukr.* 2013, 130-136.
36. I. Tkachenko, Yu. Kurioz, A. Kovalchuk, Ya. Kobzar, O. Shekera, O. Tereshchenko, V. Nazarenko and V. Shevchenko, *Molecular Crystals and Liquid Crystals*, 2020, **697**, 85-96.
37. P. M. Budd, B. S. Ghanem, S. Makhseed, N. B. McKeown, K. J. Msayib and C. E. Tattershall, *Chemical Communications*, 2004, 230-231.
38. I. Tkachenko, O. Purikova, V. Bliznyuk, O. Shekera and V. Shevchenko, *Polymer International*, 2015, **64**, 1104-1110.
39. G. Socrates, *Infrared and Raman characteristic group frequencies: tables and charts*, John Wiley & Sons, 2004.
40. M. M. Tecklenburg, D. J. Kosnak, A. Bhatnagar and D. K. Mohanty, *Journal of Raman Spectroscopy*, 1997, **28**, 755-763.
41. N. Biswas and S. Umapathy, *The Journal of Chemical Physics*, 1997, **107**, 7849-7858.
42. F. A. Miller, *Journal of Raman Spectroscopy*, 1988, **19**, 219-221.
43. D. Steele, T. Nanney and E. Lippincott, *Spectrochimica Acta*, 1966, **22**, 849-859.
44. A. I. Kovalchuk, Y. L. Kobzar, I. M. Tkachenko, A. L. Tolstov, O. V. Shekera and V. V. Shevchenko, *Journal of Molecular Structure*, 2018, **1173**, 671-678.
45. P. Sivagurunathan, K. Ramachandran and K. Dharmalingam, *Acta Physico-Chimica Sinica*, 2007, **23**, 295-298.
46. P. K. Kumar, A. Rani, L. O. Olasunkanmi, I. Bahadur, P. Venkatesu and E. E. Ebenso, *The Journal of Physical Chemistry B*, 2016, **120**, 12584-12595.
47. F. Saif, P. Undre, S. Yaseen, A. Alameen, S. Patil and P. Khirade, *Integrated Ferroelectrics*, 2019, **202**, 79-88.
48. W.C. Xu, S. Sun and S. Wu, *Angewandte Chemie International Edition*, 2019, **58**, 9712-9740.
49. B. Yang, F. Cai, S. Huang and H. Yu, *Angewandte Chemie International Edition*, 2020, **59**, 4035-4042.
50. F. Cai, B. Yang, X. Lv, W. Feng and H. Yu, *Science Advances*, 2022, **8**, eabo1626.
51. K. Ruan, Y. Guo and J. Gu, *Macromolecules*, 2021, **54**, 4934-4944.
52. X. Lei, L. Tong, H. Pan, G. Yang and X. Liu, *Journal of Materials Science: Materials in Electronics*, 2019, **30**, 18297-18305.
53. M. Wu, W. Han, C. Zhang, S. Zhang, X. Zhang, X. Chen, K. Naito, X. Yu and Q. Zhang, *Nanomaterials*, 2022, **12**, 3973.
54. I. Tkachenko, N. Belov, Yu. Yakovlev, P. Vakuliuk, O. Shekera, Yu. Yampolskii and V. Shevchenko, *Materials Chemistry and Physics*, 2016, **183**, 279-287.
55. L. Zhang, S. Maity, K. Liu, Q. Liu, R. Göstl, G. Portale, W. H. Roos and A. Herrmann, *Small*, 2017, **13**, 1701207.
56. L.W. Giles, C.F. Faul and R.F. Tabor, *Materials Advances*, 2021, **2**, 4152-4164.
57. A. Natansohn and P. Rochon, *Chemical Reviews*, 2002, **102**, 4139-4176.
58. Y. Luo, Z. Li, R. Zheng, R. Chen, Q. Yan, Q. Zhang, G. Peng, G. Zou, H. Ming and B. Zhu, *Optics Communications*, 2009, **282**, 2348-2353.
59. R. Zheng, H. Ma, Y. Zhang, X. Sun, P. Wang, H. Ming, Z. Li and Q. Zhang, *Journal of Materials Science: Materials in Electronics*, 2006, **17**, 277-280.